Silicon Nanowire Arrays Based On-Chip Thermoelectric Generators

Kam Yu Lee, David Brown, and Satish Kumar

***Abstract*— Thermoelectric generators (TEGs) can improve the net power consumption of electronic packages by generating power from the chip waste heat. In this paper, a 3-D computational model of electronic package with silicon nanowire (Si-NW)-based embedded TEGs has been developed and the effect of crucial geometric parameters, contact resistances, and thermal properties, such as pitch length and length of Si-NWs, the electrical contact resistivity at Si-NW interface, thermal contact resistivity at TEG-package interface, and filling material thermal conductivity on power generation, has been evaluated. The analysis has shown how modifying some crucial parameters from their current values in different experimental studies affect power generation, e.g., decreasing the pitch length from 400 to 200 nm doubled the power generation, increasing the Si-NW length from 1 to 8 μm increased power generation by a factor of three and decreasing contact resistivity by one order of magnitude from 1.0×10^{-11} $\Omega \cdot m^2$ enhanced the power generation by a factor of two. This paper has estimated the energy conversion efficiency of 0.15% for 8-μm long Si-NWs using the best thermoelectric properties available from different experimental studies. Finally, performance of Si-NW-based TEG has been compared against the Bi_2Te_3 superlattice-based TEGs and the crucial parameters of Si-NW TEGs have been identified which should be the focus of the future studies.**

***Index Terms*— Contact resistance, energy harvesting, silicon nanowire (Si-NW), thermoelectric generator (TEG), waste heat.**

I. INTRODUCTION

THERMOELECTRIC generators (TEGs) can harvest electrical energy when a temperature difference is applied across the two ends of the device [1]–[3]. Ultrathin thermoelectric (TE) devices have been integrated inside a microelectronic package for hotspot cooling [4]. These TE devices can also improve the net power consumption of the package by generating power from the chip waste heat [19]. Advantages of TE devices include the noise-less operation and a low risk of failure due to nonmoving parts [4]. However, their low conversion efficiency and high fabrication cost are the major disadvantages that may prevent the large-scale production and commercialization of these devices. The recent studies on embedded TE devices use bismuth telluride (Bi_2Te_3) as TE material [4]. Bi- and Te-based state-of-the-art TE materials have high figure of merit at room temperatures, but these materials are expensive and toxic, and are not CMOS-compatible [5]. Silicon nanowire (Si-NW)-based TEGs have also been investigated but have lower efficiencies [6]. To explore the ultimate power harvesting capabilities of these Si-NW TEGs, this paper investigates the effect of different crucial parameters of TEG and project the energy harvesting for the best cases of different parameters.

Silicon in its bulk form is inefficient for TEG, whereas Si-NWs have excellent TE properties, such as low thermal conductivity, a small footprint, and the ability to be manufactured in top-down technology using CMOS foundries with low production cost [6]. Nanoengineered Si-NWs with rough surfaces can have two orders of magnitude lower thermal conductivity compared with the bulk Si and its TE figure of merit can be as high as 0.5 at room temperature, which makes them very promising for use as TE materials in TEGs integrated inside a microelectronic package [7]. An individual TE element can have thousands of nanowires which are connected electrically in series and thermally in parallel. The packing density of these nanowires and the thermal properties of the filling materials inside the TEG modules have significant effect on the power generation capabilities of TEGs.

Li *et al.* [8] fabricated a Si-NW TEG of footprint 5 mm $\times$ 5 mm $\times$ 2.6 μm, filled with SiO_2, and consisting of 162 thermocouples; the power generated by this TEG is 1.5 nW from a 0.12-K temperature difference across the TEG. This is extremely low performance ($\sim$power generation). The performance of Si-NW TEG can be dramatically improved by modifying the pitch length, Si-NW length, parasitic contact resistances, or changing the filling materials [6], [8]. The measured electrical resistance of the TEG in [6] and [8] is 410 Ω. However, our calculations show that the TEG resistance is only 8.11 Ω considering the measured electrical resistance per wire ($\sim$3300 Ω) and measured electrical contact resistance per wire ($\sim$4000 Ω) in [6] and [8]. This suggests that if the device is fabricated carefully, the total resistance and energy harvesting can be significantly improved.

Former studies on Si-NW TEGs have used SiO_2 or polyimide as filling materials to fill the gap between 80- and 100-nm diameter Si-NWs and pitch of about 400 nm to enhance mechanical stability [6], [8]. SiO_2-filled Si-NW TEGs have an effective thermal conductivity of 1.6 W/m $\cdot$ K. Polyimide has a thermal conductivity of 0.14 W/m $\cdot$ K, which lowers the effective thermal conductivity of TEGs to 0.37 W/m $\cdot$ K. Lower thermal conductivity is desired to increase the temperature difference across the device.

Manuscript received August 13, 2014; revised March 15, 2015 and May 26, 2015; accepted June 9, 2015. Date of publication July 23, 2015; date of current version August 12, 2015. This work was supported by the National Science Foundation under Grant ECCS-1028569. Recommended for publication by Associate Editor M. Hodes upon evaluation of reviewers' comments.

The authors are with the G. W. Woodruff School of Mechanical Engineering, Georgia Institute of Technology, Atlanta, GA 30332 USA (e-mail: klee322@gatech.edu; dbrown3@gatech.edu; satish.kumar@me.gatech.edu).

Color versions of one or more of the figures in this paper are available online at http://ieeexplore.ieee.org.

Digital Object Identifier 10.1109/TCPMT.2015.2450234

Polyimide-filled Si-NW TEGs increased power generation by a significant factor compared with the SiO_2-filled Si-NW TEGs [8]. The Seebeck coefficient of the Si-NWs has been also reported in a wide range (39–284 μV/K) by different research groups [6], [8]. It is important to investigate the effect of this crucial TE property to evaluate the promise of Si-NW TEGs.

The contact resistance at the tip of Si-NWs can be even higher than the resistance of Si-NW itself, which will make these parasitic resistances a dominant resistance of the device [6], [8]. The parasitic contact resistances can significantly reduce the energy harvesting capability of embedded TEGs. Li et al. [9] studied the effect of electrical contact resistance on a Si-NW TE cooler and found that the effect of electrical contact resistance is critical. Lower electrical contact resistance results in greater temperature difference across the hot junction and cold junction of the device. Increase in Si-NW length can increase the available temperature difference across TEG, but also increases TEG electrical resistance. It is important to understand the effect of different geometrical and contact parameters, and TE properties on the performance limits of TEGs to correctly identify the avenues for performance enhancement.

In this paper, a 3-D computational model of electronic package with Si-NW-based embedded TEGs has been developed. The initial geometry of the Si-NW TEG was based on the experimental studies in [6] and [8]. The effect of crucial geometric parameters, contact resistances, and thermal properties on power generation has been evaluated first. Geometric parameters are important for TE device performance. Hodes [17], Redmond and Kumar [18], and Brownell and Hodes [20] have shown optimization of TE performance based on TE thickness and pellet cross-sectional area. Optimization of pellet geometry is not the focus of this paper and we keep the pellet cross-sectional area constant. Finally, the projection of energy harvesting capabilities of Si-NW TEGs has been performed using the best values of parameters reported in different experimental studies. Performance is compared against Bi_2Te_3 superlattice-based TEGs and suggestions have been provided, for future studies, to improve the parameters which seem promising in improving energy harvesting capability of embedded TEGs.

The rest of this paper is organized as follows. Section II explains the governing equations for the TEG operation, the computational model, and the validation of the model against published experimental measurements. Section III presents the key results and analysis, and Section IV concludes this paper. The nomenclature used in the paper is shown in Table I.

II. Simulation Methodology

A. Computational Model

To examine the performance of Si-NW TEGs, a 3-D computational model of electronic package with embedded Si-NW TEGs has been developed using the commercial package COMSOL. A schematic of the electronic package with TEG modules, heat spreader, thermal interface material (TIM), chip, and hotspots is shown in Fig. 1. The dimensions and material properties of the components of the system, excluding the TEG, are listed in Table II. The cross-sectional area of the TEGs was 3.5 mm × 3.5 mm and each TEG is located above a hotspot of cross-sectional area 400 μm × 400 μm. Each TEG had 32 thermocouples which was estimated using the number density of the couples in the

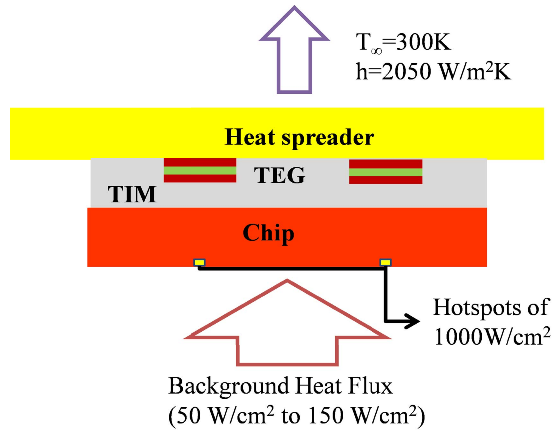

Fig. 1. Schematic of an electronic package with two TEGs. Heat spreader, chip, TIM, and TEGs are shown. Si-NW-based TEGs are attached to the back of the heat spreader. The TIM is 50-μm thick. Only half of the package is considered in COMSOL model because of symmetry across the vertical center-line through the package. Convective boundary condition (h = 2050 W/m^{2}K) is applied at top and constant heat flux boundary condition (50–150 W/cm^2) is applied at the bottom of the chip. The bottom of the chip has two hotspots of area 400 μm × 400 μm.

TABLE I
Nomenclature

Symbol	Quantity	Unit
T_H	Hot junction temperature	K
T_C	Cold junction temperature	K
N_c	Number of TE couples (n-p legs)	N/A
N_w	Number of wires per leg	N/A
S	Seebeck coefficient per leg	μV/K
V_{OC}	Seebeck voltage	V
I	Current	A
R_{TOT}	Total resistance (load and TEG)	Ω
R_L	Load resistance	Ω
R_{TEG}	TEG total resistance	Ω
$R_{contact}$	TEG electrical contact resistance	Ω
R_{elec}	Electrical resistance	Ω
$R_{elec/wire}$	Electrical resistance per wire	Ω
R''_{th}	Thermal contact resistance	K·m²/W
A_w	Wire area	m²
A_{leg}	Leg area	m²
P_{length}	Pitch length	nm
L	Si-NW length	μm
J_C	Joule heating at Si NW contact	W
J_B	Joule heat in bulk	W
W_{USEFUL}	Power at load	W
Q_{HOT}	Heat flow at hot junction	W
ρ	Mass density	kg/m³
κ	Effective thermal conductivity	W/m·K
κ_f	Filling material thermal conductivity	W/m·K
κ_w	Si-NW thermal conductivity	W/m·K
$\rho_{elec/wire}$	Si-NW electrical contact resistivity	Ω·m²

TABLE II
DIMENSIONS AND THERMAL CONDUCTIVITY OF DIFFERENT COMPONENTS OF THE ELECTRONIC PACKAGE

Component	Material	Dimensions (mm^3)	k (W/m·K)
Heat Spreader	Copper	60 x 30 x 1	400
TIM	-	11 x 13 x 0.053	1.75
Chip	Silicon	11 x 13 x 0.5	130

TABLE III
PARAMETERS OF Si-NW TEG

Properties	
Polyimide k_f (W/m·K)	0.14
SiO_2 k_f (W/m·K)	1.4
k_w (W/m·K)	7.77
L (μm)	1, 2, 8
P_{length} (nm)	200-600
$R_{elec/wire}$ (Ω)	3300
$\rho_{elec/wire}$ (Ω·m^2)	1.0x10^{-12} to 2x10^{-11}
R''_{th} (K·m^2/W)	8.0 x10^{-8} to 8.2 x10^{-6}
S (μV/K)	39 or 284

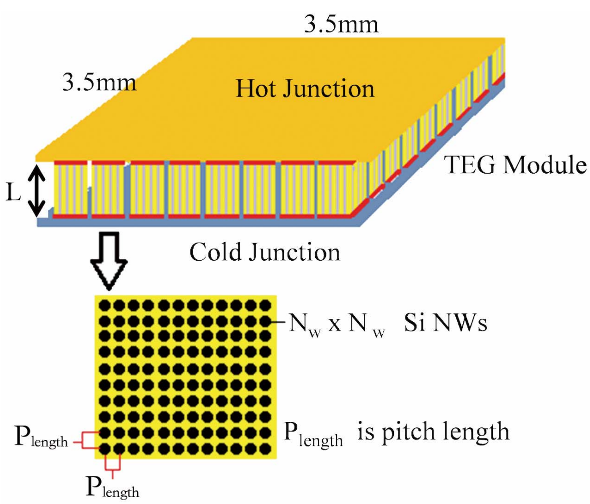

Fig. 2. Schematic of a 3.5 mm × 3.5 mm TEG module with multiple TE couples. Each leg has $N_w \times N_w$ Si-NWs of length L. Pitch length P_{length} of Si-NWs and filling material (in yellow) is shown in the bottom figure.

experimental study in [6] and [8]. Each leg was composed of an array of Si-NWs which had a diameter of 80 nm. Various parameters in the model have been studied to investigate their effects and the performance limits of the TEG. These parameters were the pitch length of Si-NWs, Si-NW length, electrical contact resistivity at Si-NW interface, thermal contact resistivity at TEG-package interface, filling materials, and background heat flux. The ranges of these parameters are listed in Table III.

Pitch length (P_{Length}) is the distance between two adjacent Si-NWs in a TE leg of TEG, as shown in Fig. 2. Increasing the pitch length decreases the total number of wires in the device as the area of a TE leg is kept constant in the present model. Si-NW length (L) is the average length of a wire (see Fig. 2), which is also the distance between the cold and hot surfaces of TEG. Increasing this length increases the temperature difference between the cold and hot surfaces (ΔT) of the TEG, which in turn increases the Seebeck voltage resulting in an overall increase in the generated power. However, an increase in Si-NW length also increases its electrical resistance; the mechanical stability of long length wires can also be a challenge. The range of P_{Length} (200–600 nm) and L (1–8 μm) is based on the experimental studies in [6] and [10]. The TEG in [6] and [8] has an aluminum top layer and a Si-NW island bottom layer each of 1-μm thickness, which sandwiches the 1-μm Si-NW layer. A similar configuration and corresponding thermal resistance was considered in the present model.

The present model has also considered all crucial thermal and electrical contact resistances in the TEG and TEG-package interface. The electrical contact resistance (R_{contact}) between the wire tip and the top aluminum layer or the Si-NW island has been incorporated in the model. Decreasing this value can significantly increase the current through the device. Thermal contact resistance (R''_{th}) at the interface between the surface of the TEG and the heat spreader has been also considered. This initial value of thermal contact resistance has been chosen to be 1×10^{-6} K $\cdot$ m^2/W which is similar to the values used in [3], [11], and [12]. Decreasing R''_{th} can increase the available ΔT across Si-NWs.

Initially, a Seebeck coefficient of 39 μV/K per leg has been used to compare results against the experimental measurements in [6] and [8]. A Seebeck coefficient of 284 μV/K per leg has been used later to assess the best possible performance of the Si-NW TEG. This high S for Si-NW has been reported in [13]. To get high mechanical stability, filling materials has been used in Si-NW TEGs [6]. The two filling materials, SiO_2 and polyimide, have been investigated in this paper. The effective thermal conductivity (κ) of the Si-NW layer is 1.6 (W/m $\cdot$ K) with SiO_2 filling material and 0.37 W/m $\cdot$ K with polyimide filling.

A convective boundary condition has been applied to the top of the heat spreader with a heat transfer coefficient of 2050 W/m^2 $\cdot$ K and ambient temperature of 300 K to consider the effect of heat sink and air cooling. A heat flux of 1000 W/cm^2 has been applied to the hotspot which is located directly underneath each TEG [11]. A background heat flux has been applied across the bottom of the entire chip and was varied from 50 to 150 W/cm^2, as shown in Fig. 1. Other outer surfaces have been assumed to be insulated.

The model assumes that the thermal properties of all materials in the package and TEGs, and the TE properties of Si-NWs are constant with respect to the temperature. This assumption is reasonable for the temperature range considered in this paper. It is assumed that all wires are well connected to their contacts on both sides. Increasing the number of meshing elements from 27 963 to 51 723 leads to less than 1% change in the power generation by TEGs; this justifies the use of 27 963 meshing elements in this paper. Temperature contour plot at the bottom of chip is shown in Fig. 3.

B. Governing Equations

The Seebeck voltage (V_{OC}) generated across the hot and cold junctions was calculated using (1), where T_H is the hot

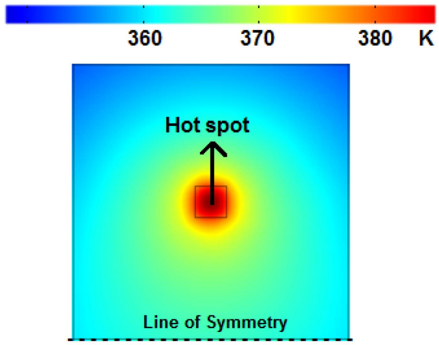

Fig. 3. Temperature contour plot at the bottom of chip. Only half of the chip with one hotspot is shown here as the temperature contours are symmetric across the dashed line between two hotspots.

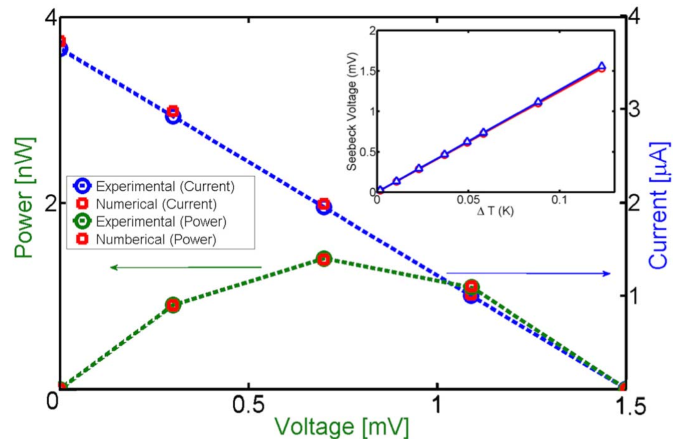

Fig. 4. Experimental data for current and power generation for different loads, when $\Delta T = 0.12$ K across Si-NW TEG from [2], are compared against the numerical results from the developed model. The maximum power generation corresponds to the case when load resistance is equal to the TEG resistance. Red markers are the numerical data. Inset shows comparison of experimental data for Seebeck voltage versus ΔT against the numerical results.

junction average temperature, T_C is the cold junction average temperature, N_C is number of thermocouples, and S is the Seebeck coefficient

$$V_{\mathrm{OC}} = 2N_c S[T_H - T_C]. \tag{1}$$

The current (I) was calculated using (2), where the total resistance (R_{TOT}) is the sum of load resistance (R_L) and TEG resistance (R_{TEG})

$$I = \frac{V_{\mathrm{OC}}}{R_{\mathrm{TOT}}} = \frac{2N_c S[T_H - T_C]}{R_L + R_{\mathrm{TEG}}}. \tag{2}$$

Useful power (W_{USEFUL}) was calculated using

$$W_{\mathrm{USEFUL}} = I^2 R_L = \left(\frac{2N_c S[T_H - T_C]}{R_L + R_{\mathrm{TEG}}}\right)^2 R_L. \tag{3}$$

The load resistance was assumed to be equal to the resistance of the TEG. The resistance of the TEG R_{TEG} was calculated using the following three equations:

$$R_{\mathrm{TEG}} = [2R_{\mathrm{contact}} + R_{\mathrm{elec}}] \tag{4}$$

where R_{contact} is the total electrical contact resistance and R_{elec} is the total electrical resistance of Si-NWs

$$R_{\mathrm{contact}} = \frac{\rho_{\mathrm{elec/wire}}}{A_w N_w} * 2 * N_c \tag{5}$$

$$R_{\mathrm{elec}} = \frac{R_{\mathrm{elec/wire}}}{N_w} * 2 * N_c. \tag{6}$$

where $R_{\mathrm{elec/wire}}$ and A_w are the resistance and area of a Si-NW, respectively, and N_w is the number of wires per leg. The hot surface of the TEG layer was adjacent to the silicon chip and cold surface was adjacent to heat spreader. The Peltier effect is a TE phenomenon that creates a temperature difference at the junction of two dissimilar materials when a voltage is applied. During TEG operation, the Peltier effect resulted from the current flowing in the TEG connected to the external load R_L. The Peltier effect at the hot and cold junctions of TEG was calculated using

$$\mathrm{Peltier}_{\mathrm{hot}} = -2N_c \mathrm{SI}T_H \tag{7}$$

$$\mathrm{Peltier}_{\mathrm{cold}} = 2N_c \mathrm{SI}T_C. \tag{8}$$

Joule heating was generated in TEGs due to the electrical current flowing through the conducting TE elements and Si-NW contacts. Bulk Joule heating (J_b) in TEG is proportional to its electrical resistance and was calculated using

$$J_b = I^2 R_{\mathrm{elec}}. \tag{9}$$

Joule heating at Si-NW end-contacts (J_c) is proportional to the electrical contact resistance which was calculated using (10). The electrical contact resistance of 3300 Ω per wire from [3] was used

$$J_c = I^2 R_{\mathrm{contact}}. \tag{10}$$

C. Validation

The computational model was validated by comparing the Seebeck voltage, current, and power through the TEG module against the experimental result from [2]. The experimental results in [2] corresponded to a TEG module sandwiched between a heat sink, Si substrate, and Si test chip. When a temperature difference of 70 K is applied across the experimental setup only 0.12 K was realized across the Si-NW TEG due to high thermal resistance of the other layers. The corresponding Seebeck voltage was 1.5 mV, which is in agreement with our model (see inset in Fig. 4). The current and power harvested by the TEG corresponding to different voltages across the load were also in good agreement with the experiments, as shown in Fig. 4.

III. Results and Discussion

A. Pitch Length and Si-NW Length

The pitch length P_{Length} and wire length L has a strong effect on the power generation capability of TEGs as they significantly affect the total thermal resistance and electrical resistance of TEGs. P_{Length} of Si-NWs in the experimental study in [6] was reported to be 400 nm. Following this value, this paper varied P_{Length} in the range of 200–600 nm to determine its effect on the power generation by TEGs.

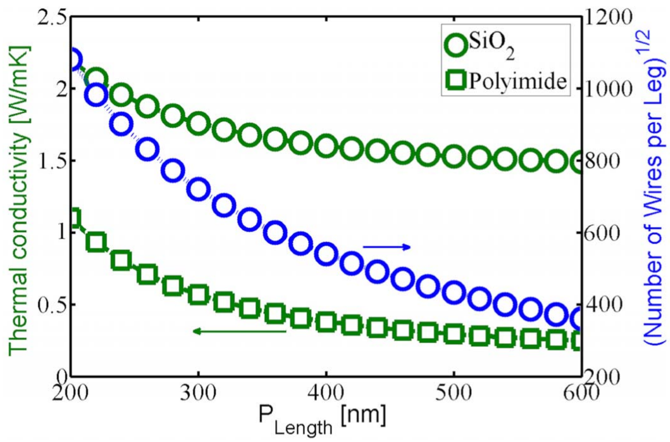

Fig. 5. Right axis: number of wires per side of the leg ($N_w^{0.5}$) versus pitch length. At 400 nm P_{Length}, there are 540 × 540 wires per leg. Increase in P_{Length} decreases the number of wires per leg. Left axis: effective thermal conductivity of the Si-NW layer decreases as pitch length increases.

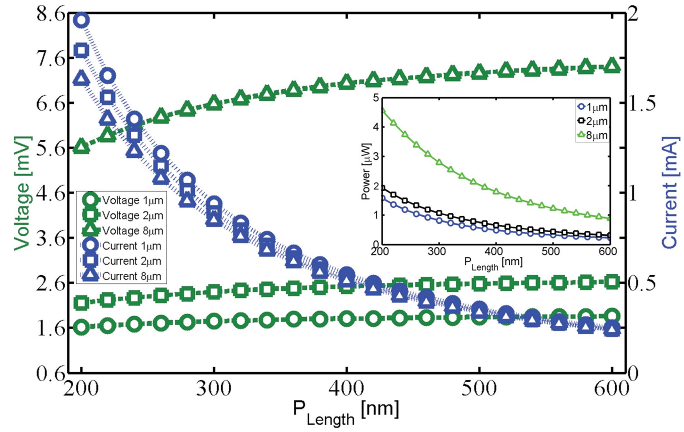

Fig. 6. Current and Seebeck voltage in a SiO$_2$-filled TEG with changing pitch length P_{Length} and Si-NW length L. Seebeck voltage increases by a factor of five when thickness increases from 1 to 8 μm. Inset shows power generated in SiO$_2$-filled TEG with changing P_{Length} and L. Useful power increase by a factor of three as L increases from 1 to 8 μm.

The inputs for this paper are shown in Table IV Case 1. Filling materials have lower thermal conductivity than Si-NW. At 400 nm P_{Length}, 540 × 540 wires per leg were considered following [6] and [8]. Increases in P_{Length} decrease number of wires and increases filling material in the Si-NW layer, consequently decreasing effective thermal conductivity of Si-NW layer, κ. An expression for κ was given by (11). Effective thermal conductivity is related to number of wires, N_w, wire thermal conductivity (κ_w), wire area (A_w), leg area (A_{leg}), and P_{Length}

$$\kappa = \frac{\kappa_w 2N_c A_w N_w + \kappa_f 2N_c[A_{\text{leg}} - A_w N_w]}{2N_c A_{\text{leg}}}$$
$$N_w = \frac{A_{\text{leg}}}{P^2_{\text{Length}}}. \tag{11}$$

Fig. 5 shows how κ decreased as P_{Length} was increased. The Seebeck voltage decreased as P_{Length} decreased due to the increased thermal conductivity of the Si-NW layer and corresponding decrease in ΔT ($T_H - T_C$). However, the current increases as P_{Length} decreases due to the decreased electrical resistance of TEG as there are more wires in a single TEG leg, as shown in Fig. 6. The relative increase in current was much higher compared with the decrease in Seebeck voltage with decreasing P_{Length}. Fig. 6 shows that the useful power doubled as P_{Length} was halved from 400 nm (540 × 540 wires per leg) to 200 nm (1080 × 1080 wires per leg) while using SiO$_2$ filling. The peak of useful power occurred at 200 nm, which was the smallest P_{Length} considered in this paper. An optimum value of the P_{Length} has not been observed in the range of P_{Length} considered, but further decreasing P_{Length} and increasing Si-NW density during TEG fabrication can be challenging and so it was not considered here as it seems unrealistic from a fabrication point of view.

Si-NW length L was varied in the range of 1–8 μm following the previous experimental studies in [6] and [10]. The inputs for this paper are shown in Table IV Case 2. Electrical resistance of Si-NW $R_{\text{elec/wire}}$ is proportional to L. Increasing L increased electrical resistance of Si-NW layer and also increased its total thermal resistance. An increase in thermal resistance lead to higher ΔT, and hence Seebeck voltage significantly increased. Seebeck voltage increased by a factor of five when L was increased from 1 to 8 μm. However, the current through TEGs did not change much due to the opposing effects of the electrical resistance and Seebeck voltage (2), as shown in Fig. 6. For P_{Length} of 200 nm, the useful power increased by a factor of three (1.6–4.8 μW) when L was increased from 1 to 8 μm. The above analysis suggests that increasing L and decreasing P_{Length} are both favorable for higher power generation. Unfortunately, fabrication of a TEG with pitch lengths less than 200 nm and Si-NW length greater than 8 μm with diameter of 80–100 nm can be challenging.

B. Filling: SiO$_2$ and Polyimide

The two filling materials, SiO$_2$ and polyimide, were investigated in this paper as they have previously been used in the fabrication of Si-NW TEGs. The thermal conductivity κ_f of polyimide (0.14 W/m·K) is an order of magnitude lower than SiO$_2$. As shown in Fig. 5, using polyimide as a filling material decreased the effective thermal conductivity of the TE layer by a factor of one-half. Fig. 7 shows that ΔT increased significantly when using polyimide as compared with a SiO$_2$ filling. The power increased by 66% when changing from a SiO$_2$ filling to a polyimide filling for a pitch length of 200 nm, as shown in Fig. 7. This observation is in agreement with experimental study in [6] and [8] and emphasizes the value of inventing and employing filling materials which can have even lower thermal conductivity than polyimide.

C. Electrical and Thermal Contact Resistances

The electrical and thermal contact resistances are significant component of the total electrical/thermal resistance of ultrathin TE devices embedded in a package and evaluation of their effect is crucial. Electrical contact resistance was measured to be 4000 Ω per wire in [6], which was higher than the resistance

TABLE IV

PROPERTIES OF THE Si-NW TEG USED FOR DIFFERENT CASES AND THE PROJECTION OF ITS POWER HARVESTING CAPABILITIES COMPARED WITH Bi_2Te_3 TEG

Case	Initial	1	2	3	4	5	Projection	Bi_2Te_3
Filling Material	SiO_2	SiO_2, Polyimide	SiO_2	SiO_2	SiO_2	Polyimide	Polyimide	--
k_f (W/m·K)	1.4	1.4, 0.14	1.4	1.4	1.4	0.14	0.14	1.2
k_w (W/m·K)	7.77	7.77	7.77	7.77	7.77	7.77	1.6	
L (μm)	1	1	1, 2, 8	1	1	1	8	8
P_{length} (nm)	400	200-600	200-600	400	400	200, 400	200	--
$R_{elec/wire}$ (Ω)	3300	3300	3300,6600,26400	3300	3300	3300	26400	--
$\rho_{elec/wire}$(Ω·m^2)	1×10^{-11}	1×10^{-11}	1×10^{-11}	2×10^{-11}, 1×10^{-12}	1×10^{-12}	1×10^{-12}	1×10^{-12}	11×10^{-12}
R''_{th} (K·m^2/W)	8.0×10^{-6}	8.0×10^{-6}	8.0×10^{-6}	8×10^{-6}	8×10^{-6} - 8×10^{-8}	8×10^{-7}	8×10^{-7}	8×10^{-7}
S (μV/K)	39	39	39	39	39	39	284	284
Result	--	Fig 5 and 7	Figure 6	Fig 8	Fig 8	Fig 9	Fig 10	--

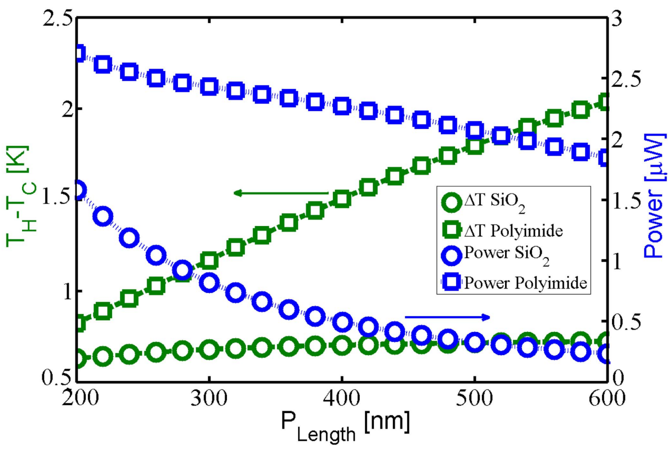

Fig. 7. Left axis: comparison of the temperature difference between hot and cold junctions of the TEG ΔT for SiO_2 and polyimide-filled TEG. Polyimide-filled TEG displayed greater ΔT than SiO_2-filled TEG due to lower effective thermal conductivity. Right axis: comparison of power generation by SiO_2 and polyimide-filled TEGs. Polyimide-filled TEG displayed a factor of two enhancement compared with SiO_2-filled TEG. Results are in agreement with [1] and [3].

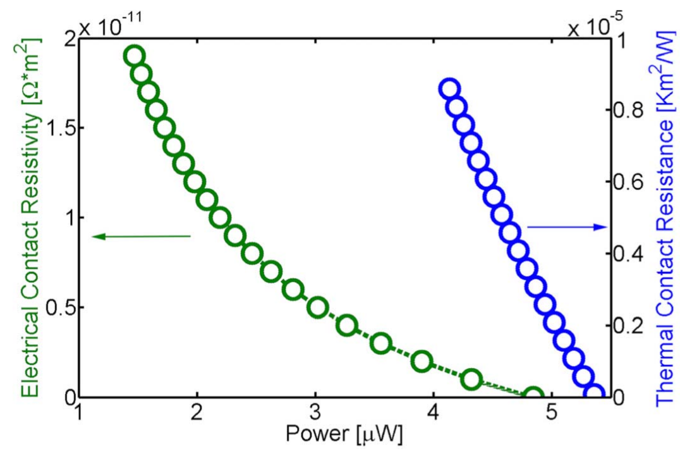

Fig. 8. Left axis: power generated versus electrical contact resistivity. Right axis: power generated versus thermal contact resistance at TEG-package interface. The result is based on 1-μm Si-NW length, polyimide-filled, 400-nm P_{Length}, and 1.0×10^{-12} $\Omega \cdot \text{m}^2$ electrical contact resistivity.

of Si-NW itself. Using (12) below, the electrical contact resistivity $\rho_{\text{elec/wire}}$ was calculated to be 1.0×10^{-11} $\Omega \cdot \text{m}^2$

$$R_{\text{wire}} = \frac{\rho_{\text{elec/wire}}}{A_w}. \tag{12}$$

In the simulation, contact resistivity was varied in the range of 1.0×10^{-12}–2×10^{-11} $\Omega \cdot \text{m}^2$. The inputs for this paper are shown in Table IV Case 3. Fig. 8 shows that decreasing the original electrical resistivity by a factor of 10 increased the power by a factor of 2. Therefore, the 1.0×10^{-12} $\Omega \cdot \text{m}^2$ value of electrical contact resistivity per wire would greatly improve the Si-NW TEG power generation capability and should be targeted during TEG fabrication.

Thermal contact resistance (R'') between the TEG and the heat spreader was reported to be 8×10^{-6} $\text{K} \cdot \text{m}^2/\text{W}$ in [4]. In the simulations, the value of this thermal contact resistance was varied from 8×10^{-8} to 8×10^{-6} $\text{K} \cdot \text{m}^2/\text{W}$. The inputs for this paper are shown in at Table IV Case 4. Fig. 8 shows that decreasing the original thermal contact resistance by a factor of 10 (8×10^{-7} $\text{K} \cdot \text{m}^2/\text{W}$) resulted in a 20% increase in power. Decreasing the original thermal contact resistance by a factor of 100 (8×10^{-8} $\text{K} \cdot \text{m}^2/\text{W}$) did not make a significant difference in power generation when compared with the resistance of 8×10^{-7} $\text{K} \cdot \text{m}^2/\text{W}$.

D. Background Heat Flux

The chip power dissipation depends on the technology and application. In this section, the effect of background heat flux on power generated by TEGs has been studied. Fig. 9 shows that increasing the background heat flux from 50 to 100 W/cm^2 resulted in increase in power generation by a factor of 5, and increasing the background heat flux to 150 W/cm^2 increased power generation by a factor of 8. Fig. 9 presents power generation comparison of a 200-nm pitch length and 400-nm pitch length for polyimide-filled and 1-μm long Si-NW TEG. The inputs for this paper are shown in Table IV Case 5. Both TEGs are modeled using the best values of electrical contact resistivity (1.0×10^{-12} $\Omega \cdot \text{m}^2$) and thermal contact resistivity (8×10^{-7} $\text{K} \cdot \text{m}^2/\text{W}$). Fig. 9 shows that the enhancement in power generation for 200-nm pitch length compared with a 400-nm pitch length increased with increasing background heat flux.

E. Projection of Energy Harvesting

In this section, projection of the energy harvesting capabilities and energy conversion efficiencies of Si-NW TEGs

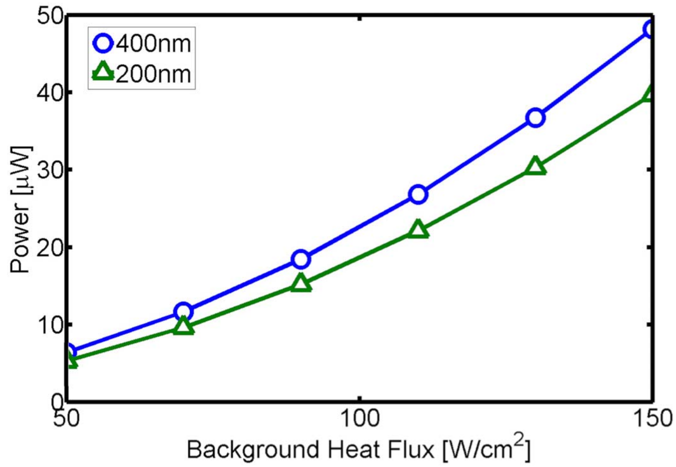

Fig. 9. Power generated versus background heat flux. The result is based on 1-μm Si-NW length, polyimide-filled, 1.0×10^{-12} $\Omega \cdot m^2$ electrical contact resistivity, and 8×10^{-7} $K \cdot m^2/W$ thermal contact resistance.

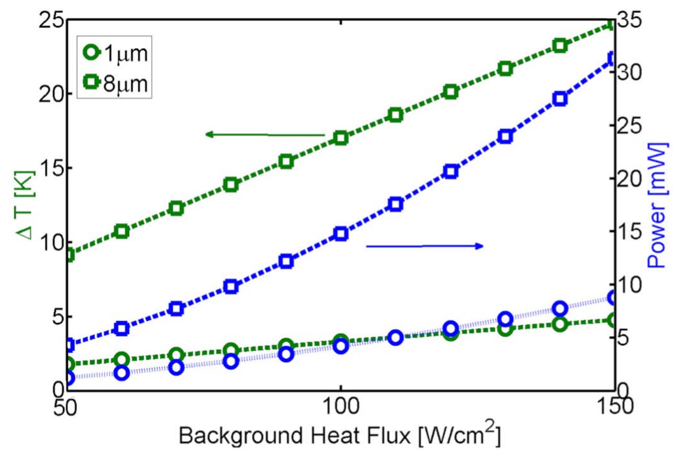

Fig. 10. Left axis: ΔT based on properties of TEG from Table IV. The results are based on Si-NW of length 1 and 8 μm, electrical contact resistivity of 1.0×10^{-12} $\Omega \cdot m^2$ and thermal contact resistance of 8×10^{-7} $K \cdot m^2/W$. Right axis: power generation based on the properties of TEG from Table IV.

has been performed using the best values of Si-NW thermal conductivity, Si-NW length, pitch length, and electrical contact resistances. These best values were based on the previous experimental studies and were separately studied in the previous sections. In addition, the Seebeck coefficient has been changed from 39 μV/K (used in previous sections) to 284 μV/K; some experimental studies have also reported this high value for Si-NW [13]. Hochbaum and Yang [14] and Lim *et al.* [16] have reported the thermal conductivity of 1.6 W/m $\cdot$ K for rough Si-NWs of diameter of the order of 50 nm. This thermal conductivity is used for the projection of energy harvesting capability. Changing the properties of the Si-NW package to these values (listed in Table IV Case Projection) increased power generation to 15 mW compared with few tens of microwatts predicted in the Sections III-C and III-D.

Using 1-μm long Si-NWs with 100 W/cm^2 background heat flux increased TEG power generation to 1 mW, while 8-μm long Si-NWs with 100 W/cm^2 background heat flux increased TEG power generation to 15 mW as shown in Fig. 10.

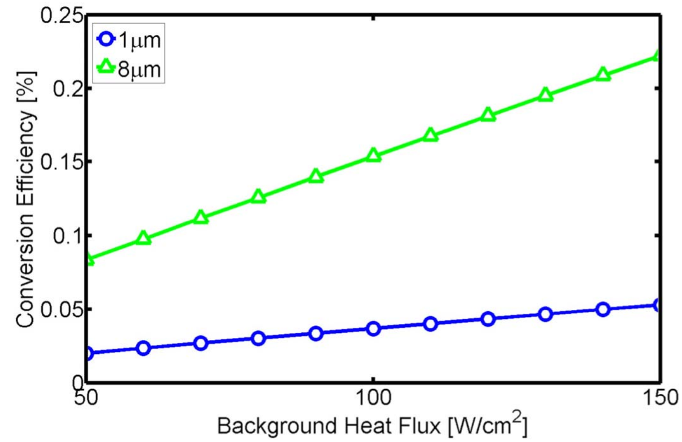

Fig. 11. Conversion efficiency of Si-NW TEG.

The energy conversion efficiency of the TEGs, which is the percentage of heat passing through the TEG converted to the useful power, for the parameters listed in Table IV (Case Projection) has also been estimated.

Fig. 11 shows a conversion efficiency of around 0.15% at a typical background heat flux of 100 W/cm^2 for Si-NWs of length 8 μm. The projected conversion efficiency of Si-NW in a typical packaging environment is low, but further improvement can be achieved by improving the properties of Si-NWs. Based on this paper the key parameters which are promising and need significant attention in experimental studies are: 1) employing Si-NW of larger length without compromising mechanical stability; 2) reducing the electrical contact resistance at Si-NW tips; and 3) reducing the thermal conductivity of Si-NWs. The present analysis also suggests that increasing Si-NW length will have better impact on power generation compared with decreasing contact resistances. In addition, an array of TEG modules can be fabricated and integrated on a chip of an electronic package to scale the energy harvesting opposed to the only two modules considered in this paper.

F. Comparison of Bi_2Te_3 and Si-NW TEGs

Bi- and Te-based superlattice materials have been used as embedded TEGs on a microelectronic chip to cool hotspots or harvest energy [11], [14]. To compare the energy harvesting capability of Si-NW TEG with a Bi_2Te_3 TEG, a model of Bi_2Te_3 TEG was developed which has similar dimensions (3.5 mm $\times$ 3.5 mm $\times$ 8 μm) and number of thermocouples (#32). The electrical contact resistance (10^{-12} $\Omega \cdot m^2$) and thermal contact resistance (8×10^{-7} $m^2 \cdot K/W$) at Bi_2Te_3–metal interface in TEG module were also kept same for a fair comparison. The properties of Bi_2Te_3 and its TEG module are listed in Table IV (Case Bi_2Te_3). The power generated by Bi_2Te_3 TEG was 74.81 mW for a background heat flux of 100 W/cm^2, which is about 5.96 times higher than the Si-NW TEG (15 mW). The conversion efficiency of Bi_2Te_3-based TEG was 0.47%, while the conversion efficiency for Si-NW-based TEG was 0.15%, as showed in Fig. 11.

The low power generation by Si-NW TEG compared with Bi_2Te_3 TEG is due to the high electrical resistivity (1448.56 mΩ compared with 30.75 mΩ) and contact resistance (21.83 mΩ compared with 0.71 mΩ) of Si-NWs (low contact area). Contact resistance was 31 times higher in Si-NW TEG and total electrical resistance was 48 times larger. Future research work should focus on lowering these electrical resistances to improve Si-NW TEG's performance.

IV. Conclusion

In summary, a 3-D model has been developed to investigate the effect of different crucial parameters of Si-NW TEG on energy harvesting from the waste heat of a microelectronic package. The analysis shows what is the promise of modifying these parameters from their current values in different experimental studies, e.g., decreasing the pitch length from 400 to 200 nm double the power generation, increasing the Si-NW length from 1 to 8 μm increases power generation by a factor of three and decreasing contact resistivity by one order of magnitude from $1.0 \times 10^{-11}\ \Omega \cdot \mathrm{m}^2$ enhances the power generation by a factor of two. The projection of energy harvesting capabilities of Si-NW TEG has been performed using the best values of Si-NW length, pitch length, electrical–thermal contact resistances, and Seebeck coefficient. The projection of power generation was 15 mW for 8-μm long Si-NWs with 100 W/cm^2 background heat flux and the corresponding energy conversion efficiency was 0.15%. Future research studies should focus on reducing pitch length by fabricating higher density Si-NW arrays, and employing rough Si-NW of larger length and reduced thermal conductivity without compromising the mechanical stability. Electrical contact resistance of the Si-NW tips are a large component of total resistance and research should aim to reduce this parameter to improve the performance of Si-NW TEGs.

References

[1] L. E. Bell, "Cooling, heating, generating power, and recovering waste heat with thermoelectric systems," *Science*, vol. 321, no. 5895, pp. 1457–1461, Sep. 2008.

[2] Q. Zhou, Z. Bian, and A. Shakouri, "Pulsed cooling of inhomogeneous thermoelectric materials," *J. Phys. D, Appl. Phys.*, vol. 40, no. 14, pp. 4376–4381, Jul. 2007.

[3] M. Redmond, K. Manickaraj, O. Sullivan, and S. Kumar, "Thermoelectric coolers for hotspot thermal management of 3D stacked chips," in *Proc. IMECE*, Denver, CO, USA, 2011, pp. 775–784.

[4] I. Chowdhury *et al.*, "On-chip cooling by superlattice-based thin-film thermoelectrics," *Nature Nanotechnol.*, vol. 4, no. 4, pp. 235–238, Apr. 2009.

[5] C. Yu, Y. S. Kim, D. Kim, and J. C. Grunlan, "Thermoelectric behavior of segregated-network polymer nanocomposites," *Nano Lett.*, vol. 8, no. 12, pp. 4428–4432, Nov. 2008.

[6] Y. Li, K. Buddharaju, B. C. Tinh, N. Singh, and S. J. Lee, "Improved vertical silicon nanowire based thermoelectric power generator with polyimide filling," *IEEE Electron Device Lett.*, vol. 33, no. 5, pp. 715–717, May 2012.

[7] A. I. Boukai, Y. Bunimovich, J. Tahir-Kheli, J.-K. Yu, W. A. Goddard, III, and J. R. Heath, "Silicon nanowires as efficient thermoelectric materials," *Nature*, vol. 451, no. 7175, pp. 168–171, Jan. 2008.

[8] Y. Li, K. Buddharaju, N. Singh, G. Q. Lo, and S. J. Lee, "Chip-level thermoelectric power generators based on high-density silicon nanowire array prepared with top-down CMOS technology," *IEEE Electron Device Lett.*, vol. 32, no. 5, pp. 674–676, May 2011.

[9] Y. Li, K. Buddharaju, N. Singh, and S. J. Lee, "Effect of electrical contact resistance in a silicon nanowire thermoelectric cooler and a design guideline for on-chip cooling applications," *J. Electron. Mater.*, vol. 42, no. 7, pp. 1476–1481, Jul. 2013.

[10] A. Stranz, A. Waag, and E. Peiner, "High-temperature performance of stacked silicon nanowires for thermoelectric power generation," *J. Electron. Mater.*, vol. 42, no. 7, pp. 2233–2238, Jul. 2013.

[11] M. P. Gupta, M.-H. Sayer, S. Mukhopadhyay, and S. Kumar, "Ultrathin thermoelectric devices for on-chip Peltier cooling," *IEEE Trans. Compon., Packag., Manuf. Technol.*, vol. 1, no. 9, pp. 1395–1405, Sep. 2011.

[12] M. P. Gupta, M.-H. S. Sayer, S. Mukhopadhyay, and S. Kumar, "On-chip Peltier cooling using current pulse," in *Proc. IEEE ITHERM*, Las Vegas, NV, USA, Jun. 2010, pp. 1–7.

[13] B. M. Curtin, E. W. Fang, and J. E. Bowers, "Highly ordered vertical silicon nanowire array composite thin films for thermoelectric devices," *J. Electron. Mater.*, vol. 41, no. 5, pp. 887–894, May 2012.

[14] A. I. Hochbaum and P. Yang, "Semiconductor nanowires for energy conversion," *Chem. Rev.*, vol. 110, no. 1, pp. 527–546, Jan. 2010.

[15] O. Sullivan, B. Alexandrov, S. Mukhopadhyay, and S. Kumar, "3D compact model of packaged thermoelectric coolers," *ASME J. Electron. Packag.*, vol. 135, no. 3, pp. 031006-1–031006-7, Jun. 2013.

[16] J. Lim, K. Hippalgaonkar, S. C. Andrews, A. Majumdar, and P. Yang, "Quantifying surface roughness effects on phonon transport in silicon nanowires," *Nano Lett.*, vol. 12, no. 5, pp. 2475–2482, 2012.

[17] M. Hodes, "Optimal pellet geometries for thermoelectric power generation," *IEEE Trans. Compon. Packag. Technol.*, vol. 33, no. 2, pp. 307–318, Jun. 2010.

[18] M. Redmond and S. Kumar, "Optimization of thermoelectric coolers for hotspot cooling in three-dimensional stacked chips," *J. Electron. Packag.*, vol. 137, no. 1, pp. 011006-1–011006-6, Mar. 2015.

[19] S. H. Choday, M. S. Lundstrom, and K. Roy, "Prospects of thin-film thermoelectric devices for hot-spot cooling and on-chip energy harvesting," *IEEE Trans. Compon., Packag., Manuf. Technol.*, vol. 3, no. 12, pp. 2059–2067, Dec. 2013.

[20] E. Brownell and M. Hodes, "Optimal design of thermoelectric generators embedded in a thermal resistance network," *IEEE Trans. Compon., Packag., Manuf. Technol.*, vol. 4, no. 4, pp. 612–621, Apr. 2012.

Kam Yu Lee received the B.S. degree in nuclear and radiological engineering from the Georgia Institute of Technology, Atlanta, GA, USA, in 2014, where she is currently pursuing the M.S. degree in mechanical engineering.

David Brown received the B.S. degree in mechanical engineering from the Georgia Institute of Technology, Atlanta, GA, USA, in 2012, where he is currently pursuing the Ph.D. degree in mechanical engineering.

His current research interests include thermal transport at interfaces in thermoelectric devices and metal/semiconductor materials.

Mr. Brown received the prestigious National Science Foundation Graduate Research Fellowship in 2013.

Satish Kumar received the Ph.D. degree in mechanical engineering and the M.S. degree in electrical and computer engineering from Purdue University, West Lafayette, IN, USA, in 2007.

He is currently an associate professor at the George W. Woodruff School of Mechanical Engineering at Georgia Institute of Technology, Atlanta, GA, USA. He has authored or co-authored over 30 journal publications.

Prof. Kumar is a recipient of the 2005 Purdue Research Foundation Fellowship, the 2012 Summer Faculty Fellowship from the Air Force Research Laboratories, the 2013 Woodruff School Teaching Fellowship, the 2014 DARPA Young Faculty Award, and the 2014 Sigma Xi Young Faculty Award.